ACCOUNTS
of chemical research

Platinum-Based Oxygen Reduction Electrocatalysts

JIANBO WU AND HONG YANG*

Departmental of Chemical & Biomolecular Engineering, University of Illinois at Urbana—Champaign, 114 Roger Adams Laboratory, MC-712, Box C-3, 600 South Matthews Avenue, Urbana, Illinois, 61801, United States

RECEIVED ON JANUARY 4, 2013

CONSPECTUS

An efficient oxygen reduction reaction (ORR) offers the potential for clean energy generation in low-temperature, proton-exchange membrane fuel cells running on hydrogen fuel and air. In the past several years, researchers have developed high-performance electrocatalysts for the ORR to address the obstacles of high cost of the Pt catalyst per kilowatt of output power and of declining catalyst activity over time. Current efforts are focused on new catalyst structures that add a secondary metal to change the d-band center and the surface atomic arrangement of the catalyst, altering the chemisorption of those oxygencontaining species that have the largest impact on the ORR kinetics and improving the catalyst activity and cost effectiveness.

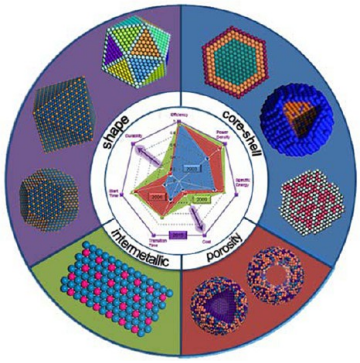

This Account reviews recent progress in the design of Pt-based ORR electrocatalysts, including improved understanding of the reaction mechanisms and the development of synthetic methods for producing catalysts with high activity and stability. Researchers have made several types of highly active catalysts, including an extended single crystal surface of Pt and its alloy, bimetallic nanoparticles, and self-supported, low-dimensional nanostructures. We focus on the design and synthetic strategies for ORR catalysts including controlling the shape (or facet) and size of Pt and its bimetallic alloys, and controlling the surface composition and structure of core–shell, monolayer, and hollow porous structures.

The strong dependence of ORR performance on facet and size suggests that synthesizing nanocrystals with large, highly reactive {111} facets could be as important, if not more important, to increasing their activity as simply making smaller nanoparticles. A newly developed carbon-monoxide (CO)-assisted reduction method produces Pt bimetallic nanoparticles with controlled facets. This CO-based approach works well to control shapes because of the selective CO binding on different, low-indexed metal surfaces. Post-treatment under different gas environments is also important in controlling the elemental distribution, especially the surface composition and the core–shell and bimetallic alloy nanostructures. Besides surface composition and facet, surface strain plays an important role in determining the ORR activity. The surface strain depends on the crystal size, the presence of an interface-lattice mismatch or twinned boundary, and between nanocrystals and extended single crystal surfaces, all of which may be factors in metal alloys. Since the common, effective reaction pathway for the ORR is a four-electron process and the surface binding of oxygen-containing species is typically the limiting step, density functional theory (DFT) calculation is useful for predicting the ORR performance over bimetallic catalysts.

Finally, we have noticed there are variations among the published values for activity and durability of ORR catalysts in recent papers. The differences are often due to the data quality and protocols used for carrying out the analysis using a rotating disk electrode (RDE). Thus, we briefly discuss some practices used in such half-cell measurements, such as sample preparation and measurement, data reliability (in both kinetic current density and durability measurement) and *iR* correction that could lead to more consistency in measured values and in evaluating catalyst performances.

1. Introduction

Molecular oxygen is essential for human survival and has been known as a natural oxidant for years, yet our ability to control the reduction of oxygen gas effectively in aqueous medium is still limited. The sluggish kinetics of reducing oxygen gas electrocatalytically in an acidic environment is a major hurdle that needs to be overcome to develop cost-effective proton exchange membrane fuel cells (PEMFCs) for various clean energy applications.[1−7] In recent years, a substantial amount of research effort has been devoted to

Published on the Web 06/28/2013 www.pubs.acs.org/accounts
10.1021/ar300359w

the design and synthesis of electrocatalysts for oxygen reduction reaction (ORR) based on both computational work and study of model systems of extended single crystals of platinum alloys.[8,9] In this Account, we focus on the design strategies of nanostructures as ORR catalysts, especially shape-controlled Pt-based nanocrystals, which are still the preferred ORR catalysts in terms of performance and stability in acidic media.

In PEMFCs, ORR takes place electro-catalytically at the cathode membrane. This reaction is rather slow, resulting in a large overpotential loss under typical hydrogen fuel cell operating conditions. Major challenge is to develop new Pt-containing catalysts that have ultrahigh activity and durability, or to create nonplatinum group metal (PGM) catalysts that are stable. The electrocatalysts developed recently include metal and alloy based nanocrystals,[6] various forms of carbon-based materials including quinone and its pyrolytic derivative,[10] transition metal macrocyclic compound,[11,12] transition metal chalcogenide,[13] transition metal carbide,[14] oxide, and pervoskite.[15] Among these classes of catalysts, Pt-based nanoparticles remain as the most practical catalysts for use in strong acidic media. Within this category of ORR catalysts, the newly developed, complex structures are often based on the theoretical analysis of compositions and structures of Pt bimetallic alloys. In several such Pt-based systems, both activity and durability are enhanced by using nanostructured, bimetallic catalysts. Although it does not always describe the electronic structures precisely, density functional theory (DFT) calculation provides important clues for the requirement of surface structures for enhanced performance in ORR. For instance, effects of non-Pt metals on the d-band electron level based on the DFT calculation offer a good reference point to explore the activity of bimetallic catalysts. It has also been recognized recently that strain shown in the Pt bimetallic structures should also play a role in determining the catalytic activity toward ORR.[16,17] Thus, a good understanding of the structure and property relationship will lead to better design of those structural factors that result in improved performance.

2. Recent Theoretical Understanding on the Oxygen Reduction

In general, oxygen reduction reaction follows two types of reaction pathways: direct four-electron reduction or two-electron reduction. The latter process involves the generation of H_2O_2 as the reaction intermediate. In the case of the four-electron reduction mechanism in acidic medium, oxygen is reduced electrocatalytically and combined with protons to form water. Operation is typically under a strong acidic environment for hydrogen fuel cells. The overall reaction for this four-electron process is given in eq 1:

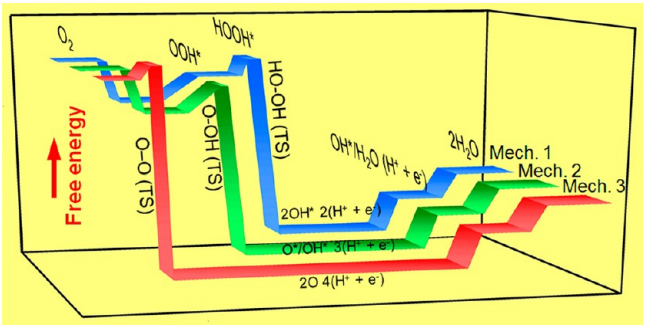

FIGURE 1. Schematic illustration of free energy levels of ORR taking place on Pt(111) surface via three different mechanisms at 0.8 V. The drawing was based on the data reported in ref 23.

$$O_2 + 4H^+ + 4e^- \rightarrow 2H_2O \quad (1)$$

The ideal standard potential, E°, for this reaction is 1.23 V. For the two-electron process, the reaction sequence and standard potentials are given by the followings:

$$O_2 + 2H^+ + 2e^- \rightarrow 2H_2O_2, \quad E^\circ = 0.67\ \text{eV} \quad (2)$$

$$H_2O_2 + 2H^+ + 2e^- \rightarrow 2H_2O, \quad E^\circ = 1.76\ \text{eV} \quad (3)$$

This pathway is generally not favored in the practice for ORR.

First principle calculations have been used for understanding the reaction mechanisms and for designing new alloy catalysts.[18−21] A recent work, which considered a variety of factors including potential bias, analyzed the energy levels for ORR with different transition states.[22] Figure 1 is a schematic illustration of relative free energy levels for the three main mechanisms under acidic conditions based on the data reported in the literature.[23] All three were identified as the four-electron processes that involve the adsorbed oxygen species, including OOH*, OH*, and HOOH*.[22,23]

At the potential between 0.8 and 0.9 V, under which PEMFCs typically operate, oxygen gas adsorbs on the surface layer of catalysts, followed by the scission of O−O bond and the formation of surface-absorbed hydroxyl groups. This process is favored among the three mechanisms. The absorbed hydroxyl further reacts with a proton to produce water. Based on this mechanism, a series of bimetallic electrocatalysts are analyzed for Pt monolayer on different non-Pt metals, such as Au, Pd, Rh, Ir, and Ru.[9] The relative activity of these catalysts toward ORR can be related to the electronic structures of the surfaces, which are modulated by the substrate metals. In particular, the d-band center (ε_d) of

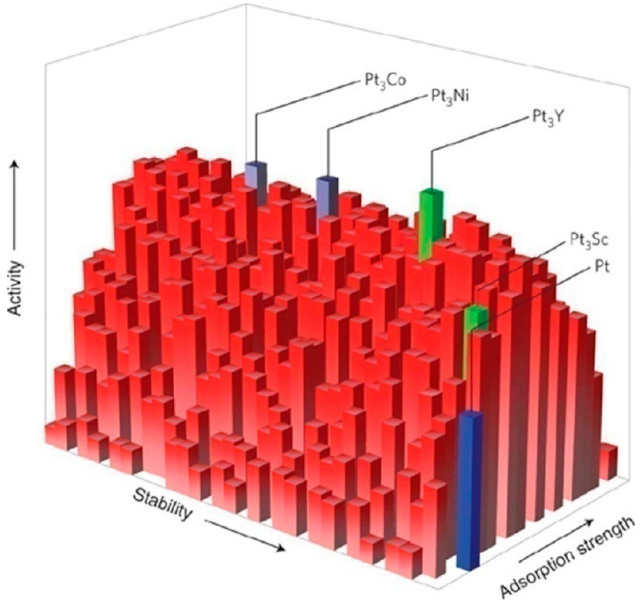

FIGURE 2. Three-dimensional activity−stability plot of metal alloy ORR catalysts (reprinted with permission from ref 24, copyright 2011 Nature Publishing Group).

surface Pt atoms and the binding energy of oxygen (BE_O) are correlated well with the experimentally determined activities.[4] The volcano-type behavior holds for these Pt bimetallic catalysts if the key reaction steps involve the O−O bond scission and O−H formation. One important prediction is the Pt monolayer of Pt_3Ni (111) surface is among the best for oxygen reduction in terms of both activity and stability.[4,21]

Some bimetallics that are active for oxygen reduction are also predicted to be stable (Figure 2). This result is intriguing because non-Pt metal constituents are generally unstable and subjected to corrosion under the strong acidic fuel cell operating conditions. One design strategy focuses on those bimetallic materials that have Pt shell as the topmost surface layer and metal alloys that possess low tendency to segregate. It is noteworthy that, based on the DFT calculation, Pt_3Y and Pt_3Sc are predicted to be both electrochemically active and stable (Figure 2).[24] Indeed, high activity and stability were observed experimentally for those Pt−Y bimetallic catalysts prepared using a sputtering technique.[25]

Facet and composition dependent ORR properties were measured on extended Pt and Pt_3Ni single crystal surfaces. The area specific activity in ORR is indeed the highest on Pt_3Ni (111) surface among the low indexed Pt mono- and bimetallic surfaces. It can be rationalized that Pt_3Ni surface has lower OH coverage than Pt, so OH species desorbs more easily from Pt_3Ni surface, followed by the adsorption of oxygen and dissociation of O−O bond. Among Pt_3Ni low-index surfaces, the order of ORR activity is as follows: (100) < (110) < (111). This order is different from structure-dependent ORR activity on Pt single-crystal surfaces, which follows the order: (100) < (111) < (110).[8] Recent results on other Pt bimetallic catalysts also show promising ORR activity.[24]

3. Single-Component Pt ORR Catalysts

The performance of ORR catalysts is typically evaluated on highly conducting carbon support. Among the monometal systems, the catalyst from E-TEK (20% Pt/C) has initial surface area of ~100 m^2/ g Pt and specific activity of 0.2 mA/ cm^2 Pt. This catalyst has often been used as a reference for comparison of both area specific and mass activities in various studies. Another class of commonly used Pt catalysts is supported on TKK porous carbon. The loading of Pt nanoparticles is able to reach 46−50% (w/w) with the electrochemical surface area reaching 65 m^2/g Pt and specific activity of 0.3−0.4 mA/cm^2 Pt. Such catalysts are typically composed particles in the size range between about 3 and 5 nm. The recently examined approach for high ORR performance is based on the control of facets using solution phase process, most noticeably those Pt nanocrystals with high indexed plane surfaces and with crystal twinning.[26,27]

In general, as-synthesized nanoparticles are bounded by low-index facets of {111} and {100} surfaces, and bridged by {110} surfaces, because the high-index facets are general active. These stable particles usually do not have a high percentage of edge, corner, and step sites, which are active. Synthesis of well-defined surface with active sites was demonstrated by an electrochemical method.[28] The tetrahexahedral (THH) Pt particles were capped by {730} facets; the type of surface structures contains relatively high numbers of atomic step edges (Figure 3).[28] The differences in reactivity among Pt catalysts are attributed in part to the binding sites presented by atoms situated at the corners and edges of nanoparticles. In cases, the reaction rate increases exponentially with the percentage of these atomic sites on the surfaces of catalysts.[29]

Besides THH Pt nanocrystals, concave nanocrystals were also made and shown to have a different set of high index facets (Figure 4a).[30] Xia and his colleagues reported the synthesis of concave cubic Pt nanoparticles enclosed by {510}, {720}, and {830} facets (Figure 4b).[31] This morphology was generated by the continuous feeding method and through the overgrowth at edges and corners along the ⟨111⟩ and ⟨110⟩ directions, respectively. These surfaces show higher activity than those low index surfaces of {100} and {111}. Detailed mechanisms for the enhanced

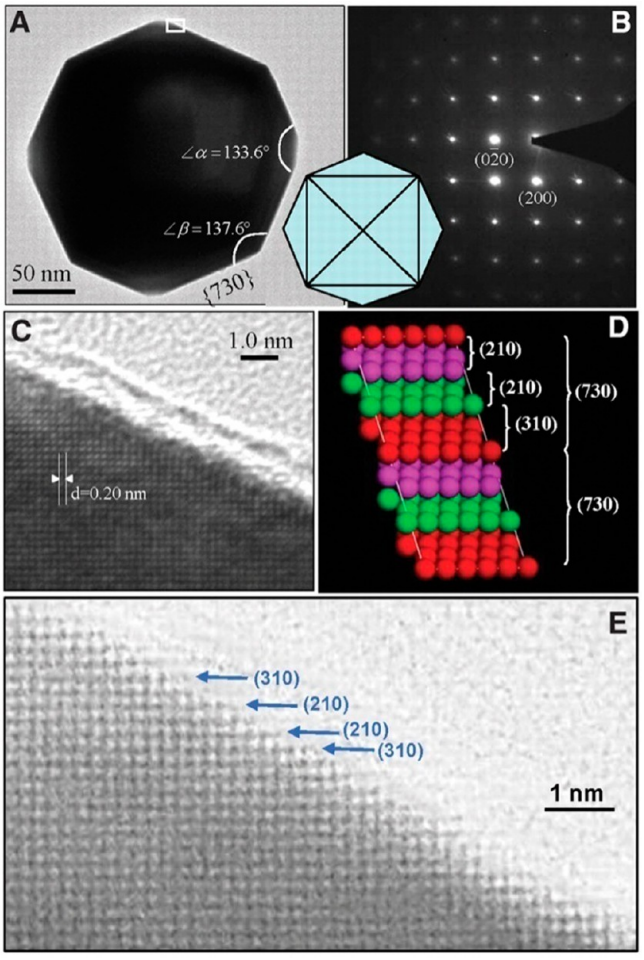

FIGURE 3. (A) TEM micrograph of THH Pt nanocrystal, (B) corresponding SAED pattern, (C) high resolution TEM micrograph, and (D) atomic model of Pt (730) plane. (E) HRTEM micrograph of a different THH Pt NC (modified with permission from ref 28, copyright 2007 American Association for the Advancement of Science).

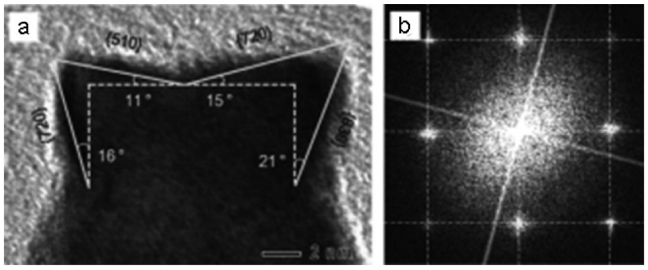

FIGURE 4. (a) HRTEM micrograph of the edge of high-index facet and atomic model of the {720} and {510} surface and (b) corresponding selective area electron diffraction (modified with permission from ref 31, copyright 2011 Wiley-VCH).

performance from high-index plane are nevertheless still not clear. It is also not clear if the mass specific activity of THH or concave cube Pt is comparable with other highly active ORR catalysts, because the Pt nanocrystals with full-grown high-index planes tend to be quite large in size.

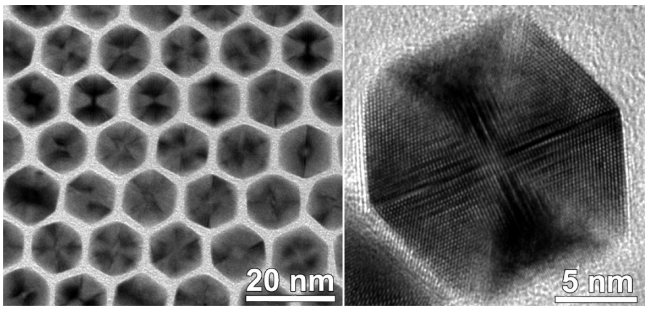

FIGURE 5. TEM micrographs of highly uniform Pt icosahedral nanocrystals (modified with permission from ref 26, copyright 2013 American Chemical Society).

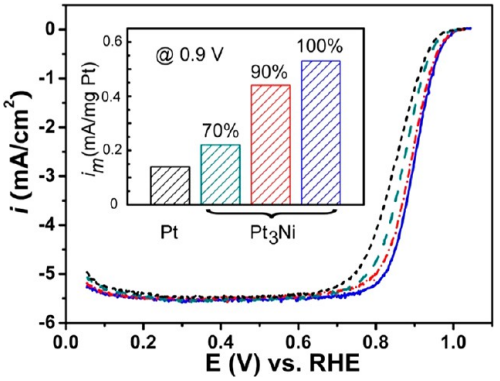

FIGURE 6. Polarization curves and (inset) correlations of the mass activities with fraction of (111) surfaces of these Pt_3Ni catalysts and reference (modified permission from ref 32, copyright 2010 American Chemical Society).

Although Pt icosahedron was bounded by the stable {111} facets, it was rarely made in a highly uniform fashion due to the greatly increased strain energy caused by the twin defects. A new approach was recently developed for the synthesis of highly uniform (95%) Pt icosahedral nanocrystals by using a hot injection-assisted GRAILS method.[26] In this approach, CO gas greatly facilitates the formation of this icosahedral shape with 30 twin boundaries (Figure 5).

4. Pt Bimetallic and Multimetallic ORR Catalysts

4.1. Shape of Bimetallic Catalysts. As discussed, Pt_3Ni (111) surface is favored for its high activity toward ORR. We observed that ORR activity for Pt_3Ni nanocrystals increases almost proportionally to the percentage of exposed {111} surfaces using cubes and other faceted crystals (Figure 6).[32,33]

The well-defined octahedral nanocrystals of Pt_3Ni and few other compositions were synthesized in organic solvents in the presence of $W(CO)_6$.[34] An approach to the synthesis of faceted Pt alloy nanocrystals was subsequently developed based on the use of CO gas.[35] This CO-based

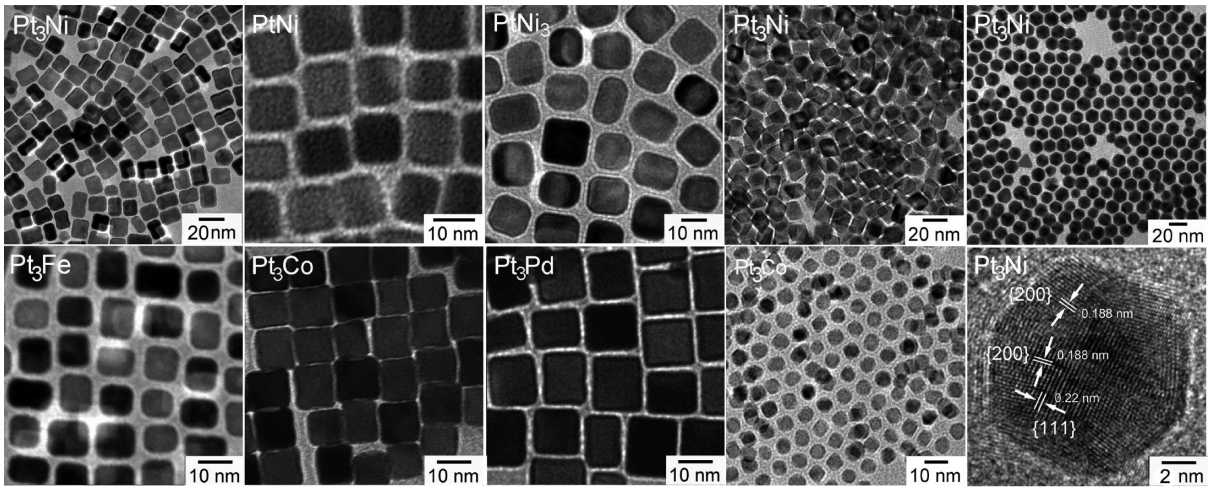

FIGURE 7. TEM images of cubic, octahedral, and icosahedral nanocrystals of various Pt bimetallic alloys.

method is capable to produce Pt bimetallic nanocrystals with a range of compositions and morphologies (Figure 7).[35] These syntheses are intriguing as they represent a platform technology where the synthesis is not as sensitive to the minor variations of synthetic mixtures as those methods without the use of this gas species. Besides cubic and octahedral shapes, the method was used to make icosahedral nanocrystals of several Pt bimetallics, an uncommon plutonic shape for Pt alloys.

In these icosahedral nanocrystals, 20 tetrahedral subunits are bounded by the {111} facets, resulting in 30 twin boundaries and a surface enclosed by the {111} facets. In comparison with octahedral nanocrystals, these Pt_3Ni icosahedral nanocrystals show a further improved ORR specific area activity of 1.83 mA/cm^2 Pt and mass activity of 0.62 A/mg Pt (Figure 8).[16] The area-specific activity of icosahedral Pt_3Ni catalysts was about 50% higher than that of the octahedral Pt_3Ni catalysts (1.26 mA/cm^2 Pt). The improvement is related to the strain-induced electronic effects. The strains in the icosahedral geometry develop as the tetrahedral subunits stretch to meet at the twin boundaries. DFT calculations showed that there was a large difference in both d-band center (0.36 eV) and hydroxyl adsorption energy (0.26 eV) for atoms on the {111} facet between Pt icosahedral and octahedral nanoparticles because of the surface strain.

For nanoparticles with size less than about 5 nm, corner and edge sites often contribute to the activity of the catalysts. It was reported that the ORR specific activity increases by a factor of 4 as the particle size changed from 1.3 to 2.2 nm.[36] This particle size dependent behavior is thought to associate with the oxygen binding energy on the different Pt

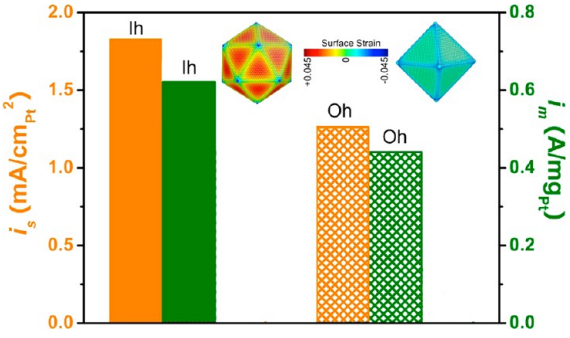

FIGURE 8. Area and mass specific ORR activities for icosahedral (Ih) and octahedral (Oh) Pt_3Ni catalysts, respectively (modified with permission from ref 16, copyright 2010 American Chemical Society).

sites on cuboctahedral particles. When nanocrystals grow large, the percentage of edge and corner sites decreases, so "trade-off" between the surface area and specific activity could lead to a size-dependent maximum of mass activity for such catalysts.

4.2. Core–Shell Nanostructured Catalysts. For better utilization of Pt, the mass activity normalized to Pt unit mass is an important benchmark. Thus, using non-Pt core and Pt shell or skin layer is another popular approach to the optimal mass activity based on the amount of Pt, besides the strategy on improving the ORR activity of uniform Pt alloy nanoparticles. Wet chemistry synthesis is quite useful in this regard, as the heterogeneous nucleation and growth are thermodynamically favored.[3] Figure 9 shows TEM micrographs of several M@Pt (M = Ag, Au, Cu and Pd) core–shell nanoparticles made based on the growth of Pt on core metal nanoparticles, which are synthesized separately and added in the solution as a particle precursors.[37,38] The TEM micrographs and elemental maps indicate there are shell

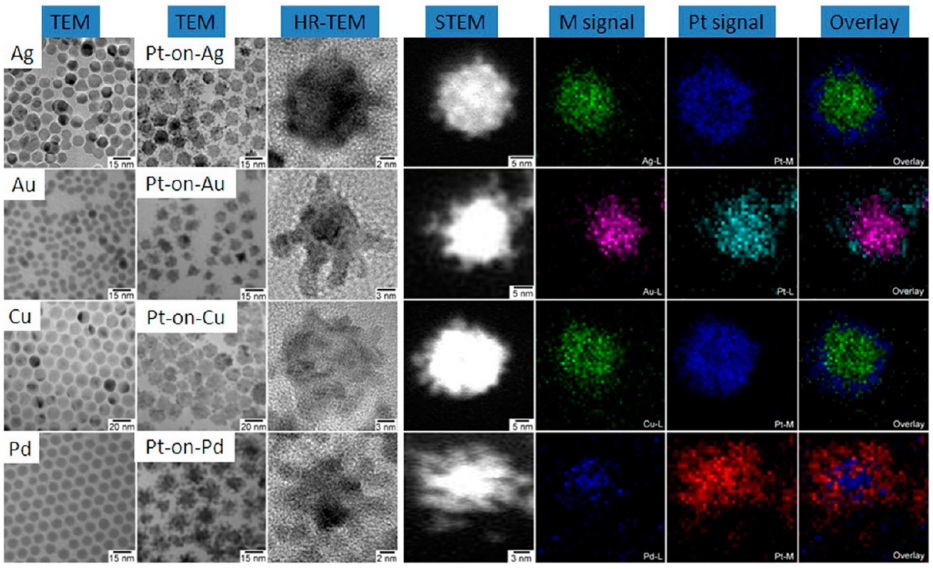

FIGURE 9. TEM micrographs and EDX maps of various Pt-on-M (M = Ag, Au, Cu, and Pd) structures.

structures of nanoparticles, but the structural detail needs to be further studied to see if Pt coating layers are in layer-by-layer or island form, or a mixture of the two.[3] Design based on core–shell configuration has been further extended to alloys in core or shell materials, which may help modulate the surface adsorption of oxygen and improve the ORR performance. In this context, $FePt_3$ bimetallic layer on (111) surface of Au nanoparticles was reported to have both high catalytic activity and good durability.[39] The surface of Pt outmost layer was also tuned by alloying Co in the Pd core. After 2000 potential cycles, a small loss of 10 mV in the half-wave potential was shown in the polarization curve for ORR measurement.[40]

Underpotential deposition (UPD) is yet another method for creating core–shell metallic nanoparticles, especially those with Pt monolayers.[41] In this electrochemical approach, copper is often used as the sacrificial layer and deposited first on the core metal via the UPD method. Pt monolayer is subsequently deposited on the metallic nanoparticles through the electrochemical replacement. Among these ORR catalysts, Pt monolayers on Pd or Pd–Au alloy cores supported on carbon (PtML/Pd/C and PtML/Pd_9Au_1/C) were shown to be extremely durable under acidic conditions, though the reported operating potentials were generally not as high as some other catalysts described in other open literatures.[42]

The Pt monolayer and its stability on metal cores were reexamined further, and the theoretical prediction[43] was compared with the experimentally determined ORR activities for a number of Pt/M(111) systems.[44,45] Three-dimensional (3D) Pt

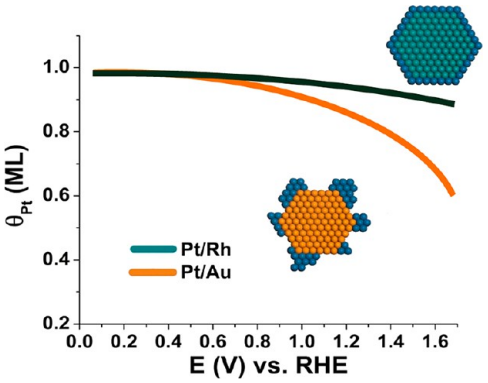

FIGURE 10. Illustration of Pt coverage θ_{Pt} as a function of increasing potentials for growth of Pt/Rh(111) and Pt/Au(111) (redrawn based on the data from ref 46).

islandlike structures were obtained through the redox displacement, instead of the uniform two-dimensional (2D) monolayers predicted. A 3D Pt/Rh(111) sample was used to compare with Pt/Au(111). The result indicated that Pt could not be readily grown on Au readily in a layer-by-layer fashion, because Au has a significantly lower surface energy than Pt.[46] The surface energy and cohesion energy strongly influence the redox chemistry of Pt islands at potentials above 1.0 V (Figure 10), where Pt oxides and hydrated Pt cations become thermodynamically stable. Such conditions are used in various fuel cell operating scenarios and contribute significantly to catalyst degradation.

4.3. Other Pt Nanostructured Catalysts. Catalysts from Dealloy Process. Electrochemical removal of more reactive metals from platinum-based alloys is used to make core–shell or other complex nanoparticles with surface rich

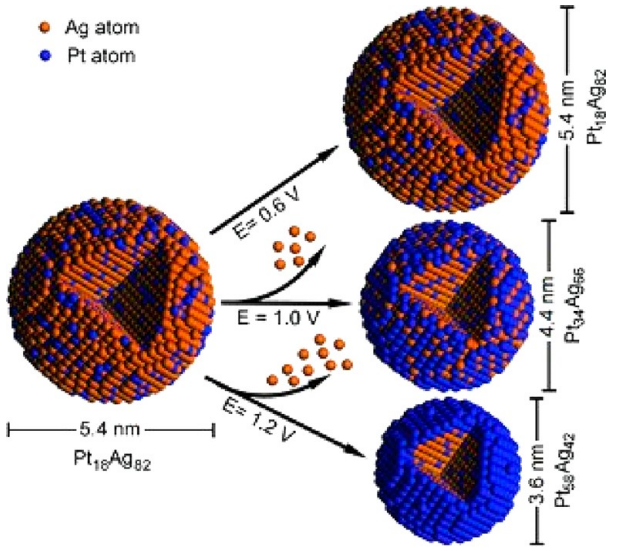

FIGURE 11. Schematic illustration of compositional and structural changes of PtAg alloy nanoparticles made by controlled dissolution of Ag metal (modified with permission from ref 47, copyright 2010 Wiley-VCH).

in Pt (Figure 11). This method is based on the difference in redox potentials between the metal pairs. For instance, PtAg alloy nanoparticles rich in Pt at the surface were produced through selective electrochemical removal of Ag atoms under different potentials.[47] The size-reduced PtAg alloy nanoparticles with surface rich in Pt were generated when potential was cycled between 0 and 1.2 V. In CuCoPt ternary particles, Cu was preferably removed from the CuCoPt particles after potential cycles to form the nanostructures having Pt and Co enriched surfaces and compressed surface strain, which enhanced the ORR activity.[48]

Supportless Catalysts of Pt Nanostructures. Besides the core–shell structures, hollow porous or skeleton structures have been examined as other morphologies that show good performance in activity or stability. Templating method based on porous anodic aluminum oxide or galvanic replacement have been used for the preparation of hollow structures for decades.[49] PtPd and PtCuCoNi nanotubes were made based on the above synthetic mechanism.[50,51] Those porous nanotubes have relatively low Pt content and high surface area, which are expected to utilize Pt for catalytic reactions effectively. The hollow and porous structures have also been used as self-supporting catalysts in order to eliminate the use of carbon support,[50] thus the degradation related to the corrosion of carbon.

One issue which may help to further understand the reaction mechanism, thus the design principles for making better catalysts is the surface structural change under reaction conditions. For bimetallic alloy catalysts in gas phase environments, surface composition may change when exposed to different gases, such as CO, H_2 and O_2.[52,53] This change is reversible and the evolution in surface composition and chemical state under catalytic reactions were studied by X-ray photoelectron spectroscopy (XPS). As an example, the surface composition of the bimetallic nanoparticles (e.g., PtCu) can be controlled by introducing the reducing gas (e.g., CO) on the catalysts surface.[53] It was hypothesized that Cu in PtCu is pulled to surface by adsorbed CO. The principle could be relevant to engineer the surface composition of Pt-M (M = Co, Cu, and Ni) bimetallic catalysts to modulate the oxygen adsorption and reduction.[54,55] Multilayered Pt-skin surfaces were created with an acid solution, followed by an annealing treatment. Such structures show enhanced ORR activity over 2.5 mA/cm^2 Pt.[54]

5. Studying the Performance of ORR Catalysts

Measurements of ORR activity are often carried out by using either rotating disk electrode (RDE) or membrane electrode assembly (MEA). RDE is designed for measuring the catalyst performance based on a half-cell configuration, such as ORR through the cathodic half reaction. The MEA is the essential component of a fuel cell stack. An MEA is consisted of both anodic and cathodic electrodes, diffusion media (or substrates), and a proton-conducting membrane.[2] MEA is particularly valuable for evaluating the catalyst performance in practical applications of PEMFCs for electric vehicles. The measurement based on MEA measurement however, is not trivial and high-level fabrication and measurement apparatuses are often not readily accessible to the general research laboratories. On the other hand, RDE method has the advantage of easy access and versatility; thus is popular in studying the performance of new ORR catalysts. Correlations in ORR performances between RDE and MEA measurements are shown to be comparable if sufficient care is taken place, but not always straightforward.[2,56] Thus, precaution is necessary in making the ORR measurement and in the interpretation of intrinsic activity of catalysts, because under the strong acidic condition the obtained values are often sensitive to measurement conditions, such as oxygen concentration, and preparation techniques including the dispersal of catalysts on RDE, and whether *iR*-correction is used.

In general, the quality of catalyst film deposited on the surface of RDE is important for obtaining accurate data on ORR activity.[57] The proper amount of Pt loading on the support, and uniformity in both catalyst ink and electrode

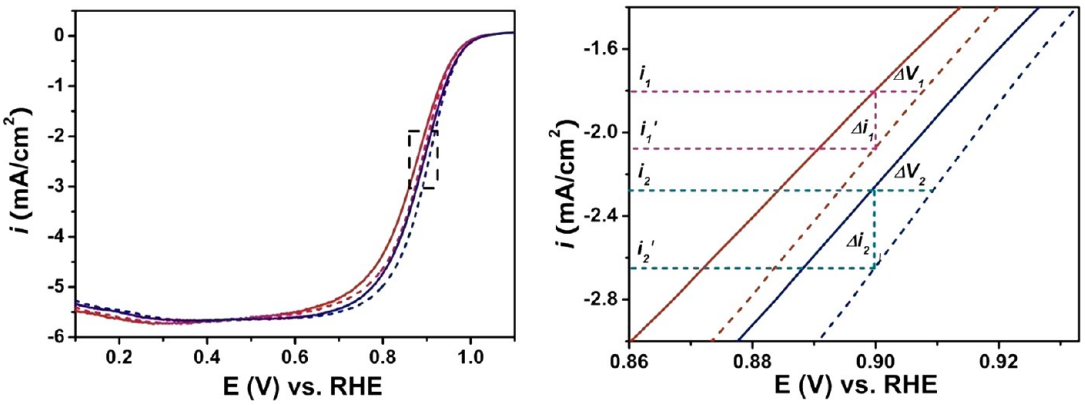

FIGURE 12. ORR polarization curves of cubic (red) and octahedral (blue) Pt_3Ni nanoparticles before (solid) and after (dashed) *iR* compensation.

film can all greatly affect the values obtained. In one popular method for making the catalyst ink, water, isopropanol, and Nafion are used. The isopropanol helps the dispersity of catalyst particles in aqueous mixtures. Prewet RDE may be necessary for improving the uniformity of the thin-film of catalyst layers. Drying of catalyst layers may be accomplished by a gentle flow of nitrogen or argon gas. In the ORR measurement, reference electrode (Ag/AgCl or hydrogen reference) should be placed in a separate compartment in order to avoid the effect of ionic species. Empirically, for a properly prepared electrode, the polarization curves should be fairly flat in the potential range between 0.2 and 0.5 V (vs RHE) and the curve density in this range should approach to 5.5 mA/cm^2.

Under the potentiostatic condition, it is assumed that the potential drop across the interface region at the working electrode is the same as the potential applied between the reference electrode and working electrode. Further this assumption needs to be corrected by considering the *iR* drops at the electrodes, which come from electrolyte resistance. The resistance can be measured via the three-electrode test, in which all three electrodes connected in O_2-saturated, acidic solution based on the equation:

$$E_{cell} = E_{ideal} - \Delta V_{ohm} = E_{ideal} - i_{cell}R \qquad (4)$$

where E_{cell} is the measured potential, E_{ideal} represents the potential without *iR* drop, and *R* is the resistance between the reference electrode and working electrode. In the literature, activities have been reported with or without *iR*-correction. Figure 12 shows *iR*-corrected current densities for two Pt_3Ni catalysts with cubic (1) and octahedral (2) morphologies that have different current densities ($i_2 > i_1$). If the resistance between working and reference electrodes are the same, compensation due to the *iR* drop is larger for the more active catalyst than that for the less active one ($\Delta V_2 > \Delta V_1$). If the slopes are similar in the polarization curves for these two catalysts, the ORR polarization curve is shifted more positively for the catalyst with high activity. Figure 12 shows the ORR polarization curves for Pt_3Ni cubic and octahedral catalysts. There is a 8-mV shift for the cubes and a 10-mV shift for octahedra. Noticeably, a change of 8−10 mV in polarization curve at ~0.9 V is equivalent to a current density change of 0.26 mA/cm^2 (or 14%) increase for the cubes and 0.36 mA/cm^2 (or 16%) for the octahedra. With *iR* correction, the kinetic current density increase further by 25% for both samples. In general, *R* values vary depending on the setup for the measurement, (e.g., electrolyte, distance between working electrode and reference electrode and so on) and are determined by the electrochemical impedance spectroscopy (EIS) technique. In acidic medium, *R* value is typically small so the ORR data are often reported without the *iR* correction in literature.

6. Concluding Remarks

In the past several years, major progresses have been made in understanding the fundamentals of oxygen reduction reaction with respect to the design of Pt and its bimetallic catalysts. The design strategies can be classified into the following categories: (a) alloying second metal with Pt to modify the surface structure and to change the d-band center, thus the chemisorption of oxygen species; (b) controlling the most active surface through the optimization of size; (c) making the shell rich in Pt using transition metals as a core or based on a hollow structure; (d) using alternative materials other than carbon as the catalyst support; and (e)

synthesizing three-dimensional structures as self-supported catalysts to eliminate the usage of carbon. Several Pt-free materials have also been identified to show excellent ORR activity, most noticeably N-containing and/or graphene-based compounds. For non-Pt ORR catalysts, chalcogenide-type materials, in which the transition metal binds with polypyrrole-XC72 (PPY-XC72) to form the nanocomposite, and N-doped graphene show promise in high activities. It appears, though the Pt group metals will continue to play an important role as the choice for the most active and stable ORR catalysts under acidic conditions and among Pt-based ORR catalysts, bi- or multimetallic alloys are particularly promising.

This work is supported by the NSF (CHE-1213926) and a start-up fund from University of Illinois. Data from our group have been produced also by support from the NSF (DMR-0449849), NYSERDA, and General Motors. We thank Dr. Zhenmeng Peng for his contribution to Figures 9 and our able colleagues whose work is presented in this Account.

BIOGRAPHICAL INFORMATION

Dr. Jianbo Wu was born in Zhejiang, China, in 1982. He received his B.S. degree in Materials Science and Engineering in 2005 and his M.S. degree in Materials Physics and Chemistry, both from Zhejiang University in 2007. He then came to University of Rochester to pursue his Ph.D. degree under the direction of Professor Hong Yang. He received the Elon Huntington Hooker Fellowship in 2011. His doctoral research is focused on colloidal chemistry, shape control of platinum-based alloys and intermetallics, and their applications as facet-dependent electrocatalysts.

Prof. Hong Yang received his B.Sc. degree from Tsinghua University in 1989, M.Sc. degree from University of Victoria in 1994, and Ph.D. degree from University of Toronto in 1998. After working at Harvard University as an NSERC postdoctoral fellow, he started his independent research at University of Rochester and went through his academic rank there. He joined the faculty of University of Illinois at Urbana−Champaign as a Professor of Chemical and Biomolecular Engineering in January 2012. Dr. Yang is an NSERC Canada Doctoral Prize winner and an NSF CAREER Award recipient. He is a Section Editor on Nanotechnology for *Current Opinion in Chemical Engineering* and serves on the editorial boards of *Nano Today* and other journals. His research interests include shape control of nanocrystals, surface modification, material design for catalysis, and nanomaterials for energy and biological applications.

FOOTNOTES

*To whom correspondence should be addressed. E-mail: hy66@illinois.edu.
The authors declare no competing financial interest.

REFERENCES

1 Wagner, F. T.; Lakshmanan, B.; Mathias, M. F. Electrochemistry and the Future of the Automobile. *J. Phys. Chem. Lett.* **2010**, *1*, 2204–2219.
2 Gasteiger, H. A.; Kocha, S. S.; Sompalli, B.; Wagner, F. T. Activity benchmarks and requirements for Pt, Pt-alloy, and non-Pt oxygen reduction catalysts for PEMFCs. *Appl. Catal., B* **2005**, *56*, 9–35.
3 Peng, Z. M.; Yang, H. Designer Platinum Nanoparticles: Control of Shape, Composition in Alloy, Nanostructure and Electrocatalytic Property. *Nano Today* **2009**, *4*, 143–164.
4 Norskov, J. K.; Bligaard, T.; Rossmeisl, J.; Christensen, C. H. Towards the Computational Design of Solid Catalysts. *Nat. Chem.* **2009**, *1*, 37–46.
5 Debe, M. K. Electrocatalyst Approaches and Challenges for Automotive Fuel Cells. *Nature* **2012**, *486*, 43–51.
6 Yu, W.; Porosoff, M. D.; Chen, J. G. Review of Pt-Based Bimetallic Catalysis: From Model Surfaces to Supported Catalysts. *Chem. Rev.* **2012**, *112*, 5780–5817.
7 Chen, J. Y.; Lim, B.; Lee, E. P.; Xia, Y. N. Shape-Controlled Synthesis of Platinum Nanocrystals for Catalytic and Electrocatalytic Applications. *Nano Today* **2009**, *4*, 81–95.
8 Stamenkovic, V. R.; Fowler, B.; Mun, B. S.; Wang, G. F.; Ross, P. N.; Lucas, C. A.; Markovic, N. M. Improved Oxygen Reduction Activity on $Pt_3Ni(111)$ via Increased Surface Site Availability. *Science* **2007**, *315*, 493–497.
9 Stamenkovic, V.; Mun, B. S.; Mayrhofer, K. J. J.; Ross, P. N.; Markovic, N. M.; Rossmeisl, J.; Greeley, J.; Norskov, J. K. Changing the Activity of Electrocatalysts for Oxygen Reduction by Tuning the Surface Electronic Structure. *Angew. Chem., Int. Ed.* **2006**, *45*, 2897–2901.
10 Fournier, J.; Lalande, G.; Cote, R.; Guay, D.; Dodelet, J. P. Activation of Various Fe-based Precursors on Carbon Black and Graphite Supports to Obtain Catalysts for the Reduction of Oxygen in Fuel Cells. *J. Electrochem. Soc.* **1997**, *144*, 218–226.
11 Dodelet, J. P. In *N4-Macrocyclic Metal Complexes*; Zagal, J. H., Bedioui, F., Dodelet, J. P., Eds.; Springer: New York, 2006; p 83.
12 Brushett, F. R.; Thorum, M. S.; Lioutas, N. S.; Naughton, M. S.; Tornow, C.; Jhong, H.-R. M.; Gewirth, A. A.; Kenis, P. J. A. A Carbon-Supported Copper Complex of 3,5-Diamino-1,2,4-triazole as a Cathode Catalyst for Alkaline Fuel Cell Applications. *J. Am. Chem. Soc.* **2010**, *132*, 12185–12187.
13 Gao, M. R.; Gao, Q.; Jiang, J.; Cui, C. H.; Yao, W. T.; Yu, S. H. A Methanol-Tolerant $Pt/CoSe_2$ Nanobelt Cathode Catalyst for Direct Methanol Fuel Cells. *Angew. Chem., Int. Ed.* **2011**, *50*, 4905–4908.
14 Esposito, D. V.; Chen, J. G. Monolayer Platinum Supported on Tungsten Carbides as Low-Cost Electrocatalysts: Opportunities and Limitations. *Energy Environ. Sci.* **2011**, *4*, 3900–3912.
15 Suntivich, J.; May, K. J.; Gasteiger, H. A.; Goodenough, J. B.; Shao-Horn, Y. A Perovskite Oxide Optimized for Oxygen Evolution Catalysis from Molecular Orbital Principles. *Science* **2011**, *334*, 1383–1385.
16 Wu, J.; Qi, L.; You, H.; Gross, A.; Li, J.; Yang, H. Icosahedral Platinum Alloy Nanocrystals with Enhanced Electrocatalytic Activities. *J. Am. Chem. Soc.* **2012**, *134*, 11880–11883.
17 Strasser, P.; Koh, S.; Anniyev, T.; Greeley, J.; More, K.; Yu, C. F.; Liu, Z. C.; Kaya, S.; Nordlund, D.; Ogasawara, H.; Toney, M. F.; Nilsson, A. Lattice-Strain Control of the Activity in Dealloyed Core-Shell Fuel Cell Catalysts. *Nat. Chem.* **2010**, *2*, 454–460.
18 Vang, R. T.; Honkala, K.; Dahl, S.; Vestergaard, E. K.; Schnadt, J.; Laegsgaard, E.; Clausen, B. S.; Norskov, J. K.; Besenbacher, F. Controlling the Catalytic Bond-Breaking Selectivity of Ni Surfaces by Step Blocking. *Nat. Mater.* **2005**, *4*, 160–162.
19 Kandoi, S.; Greeley, J.; Sanchez-Castillo, M. A.; Evans, S. T.; Gokhale, A. A.; Dumesic, J. A.; Mavrikakis, M. Prediction of Experimental Methanol Decomposition Rates on Platinum from First Principles. *Top. Catal.* **2006**, *37*, 17–28.
20 Gokhale, A. A.; Dumesic, J. A.; Mavrikakis, M. On the Mechanism of Low-Temperature Water Gas Shift Reaction on Copper. *J. Am. Chem. Soc.* **2008**, *130*, 1402–1414.
21 Greeley, J.; Mavrikakis, M. Alloy Catalysts Designed from First Principles. *Nat. Mater.* **2004**, *3*, 810–815.
22 Norskov, J. K.; Rossmeisl, J.; Logadottir, A.; Lindqvist, L.; Kitchin, J. R.; Bligaard, T.; Jonsson, H. Origin of the Overpotential for Oxygen Reduction at a Fuel-Cell Cathode. *J. Phys. Chem. B* **2004**, *108*, 17886–17892.
23 Nilekar, A. U.; Mavrikakis, M. Improved Oxygen Reduction Reactivity of Platinum Monolayers on Transition Metal Surfaces. *Surf. Sci.* **2008**, *602*, L89–L94.
24 Mayrhofer, K. J. J.; Arenz, M. Log on for New Catalysts. *Nat. Chem.* **2009**, *1*, 518–519.
25 Hwang, S. J.; Kim, S.-K.; Lee, J.-G.; Lee, S.-C.; Jang, J. H.; Kim, P.; Lim, T.-H.; Sung, Y.-E.; Yoo, S. J. Role of Electronic Perturbation in Stability and Activity of Pt-Based Alloy Nanocatalysts for Oxygen Reduction. *J. Am. Chem. Soc.* **2012**, *134*, 19508–19511.
26 Zhou, W.; Wu, J.; Yang, H. Highly Uniform Platinum Icosahedra Made by Hot Injection-Assisted GRAILS Method. *Nano Lett.* **2013**, *13*, 2870–2874.
27 Kang, Y.; Pyo, J. B.; Ye, X.; Diaz, R. E.; Gordon, T. R.; Stach, E. A.; Murray, C. B. Shape-Controlled Synthesis of Pt Nanocrystals: The Role of Metal Carbonyls. *ACS Nano* **2012**, *7*, 645–653.
28 Tian, N.; Zhou, Z. Y.; Sun, S. G.; Ding, Y.; Wang, Z. L. Synthesis of Tetrahexahedral Platinum Nanocrystals with High-Index Facets and High Electro-Oxidation Activity. *Science* **2007**, *316*, 732–735.
29 Narayanan, R.; El-Sayed, M. A. Shape-Dependent Catalytic Activity of Platinum Nanoparticles in Colloidal Solution. *Nano Lett.* **2004**, *4*, 1343–1348.

30 Zhang, J.; Langille, M. R.; Personick, M. L.; Zhang, K.; Li, S.; Mirkin, C. A. Concave Cubic Gold Nanocrystals with High-Index Facets. *J. Am. Chem. Soc.* **2010**, *132*, 14012–14014.

31 Yu, T.; Kim, D. Y.; Zhang, H.; Xia, Y. Platinum Concave Nanocubes with High-Index Facets and Their Enhanced Activity for Oxygen Reduction Reaction. *Angew. Chem., Int. Ed.* **2011**, *50*, 2773–2777.

32 Wu, J.; Zhang, J.; Peng, Z.; Yang, S.; Wagner, F. T.; Yang, H. Truncated Octahedral Pt_3Ni Oxygen Reduction Reaction Electrocatalysts. *J. Am. Chem. Soc.* **2010**, *132*, 4984–4985.

33 Wu, J.; Yang, H. Synthesis and Electrocatalytic Oxygen Reduction Properties of Truncated Octahedral Pt_3Ni Nanoparticles. *Nano Res.* **2011**, *4*, 72–82.

34 Zhang, J.; Yang, H. Z.; Fang, J. Y.; Zou, S. Z. Synthesis and Oxygen Reduction Activity of Shape-Controlled Pt_3Ni Nanopolyhedra. *Nano Lett.* **2010**, *10*, 638–644.

35 Wu, J. B.; Gross, A.; Yang, H. Shape and Composition-Controlled Platinum Alloy Nanocrystals Using Carbon Monoxide as Reducing Agent. *Nano Lett.* **2011**, *11*, 798–802.

36 Shao, M.; Peles, A.; Shoemaker, K. Electrocatalysis on Platinum Nanoparticles: Particle Size Effect on Oxygen Reduction Reaction Activity. *Nano Lett.* **2011**, *11*, 3714–3719.

37 Peng, Z.; Yang, H. Synthesis and Oxygen Reduction Electrocatalytic Property of Pt-on-Pd Bimetallic Heteronanostructures. *J. Am. Chem. Soc.* **2009**, *131*, 7542–7543.

38 Peng, Z.; Wu, J.; Yang, H. Synthesis and Oxygen Reduction Electrocatalytic Property of Platinum Hollow and Platinum-on-Silver Nanoparticles. *Chem. Mater.* **2009**, *22*, 1098–1106.

39 Wang, C.; van der Vliet, D.; More, K. L.; Zaluzec, N. J.; Peng, S.; Sun, S.; Daimon, H.; Wang, G.; Greeley, J.; Pearson, J.; Paulikas, A. P.; Karapetrov, G.; Strmcnik, D.; Markovic, N. M.; Stamenkovic, V. R. Multimetallic Au/$FePt_3$ Nanoparticles as Highly Durable Electrocatalyst. *Nano Lett.* **2010**, *11*, 919–926.

40 Wang, D.; Xin, H. L.; Yu, Y.; Wang, H.; Rus, E.; Muller, D. A.; Abruña, H. D. Pt-Decorated PdCo@Pd/C Core−Shell Nanoparticles with Enhanced Stability and Electrocatalytic Activity for the Oxygen Reduction Reaction. *J. Am. Chem. Soc.* **2010**, *132*, 17664–17666.

41 Adzic, R. R.; Zhang, J.; Sasaki, K.; Vukmirovic, M. B.; Shao, M.; Wang, J. X.; Nilekar, A. U.; Mavrikakis, M.; Valerio, J. A.; Uribe, F. Platinum Monolayer Fuel Cell Electrocatalysts. *Top. Catal.* **2007**, *46*, 249–262.

42 Sasaki, K.; Naohara, H.; Cai, Y.; Choi, Y. M.; Liu, P.; Vukmirovic, M. B.; Wang, J. X.; Adzic, R. R. Core-Protected Platinum Monolayer Shell High-Stability Electrocatalysts for Fuel-Cell Cathodes. *Angew. Chem., Int. Ed.* **2010**, *49*, 8602–8607.

43 Greeley, J.; Stephens, I. E. L.; Bondarenko, A. S.; Johansson, T. P.; Hansen, H. A.; Jaramillo, T. F.; Rossmeisl, J.; Chorkendorff, I.; Norskov, J. K. Alloys of Platinum and Early Transition Metals as Oxygen Reduction Electrocatalysts. *Nat. Chem.* **2009**, *1*, 552–556.

44 Zhang, J. L.; Vukmirovic, M. B.; Xu, Y.; Mavrikakis, M.; Adzic, R. R. Controlling the Catalytic Activity of Platinum-Monolayer Electrocatalysts for Oxygen Reduction with Different Substrates. *Angew. Chem., Int. Ed.* **2005**, *44*, 2132–2135.

45 Brankovic, S. R.; Wang, J. X.; Adzic, R. R. Metal Monolayer Deposition by Replacement of Metal Adlayers on Electrode Surfaces. *Surf. Sci.* **2001**, *474*, L173–L179.

46 Friebel, D.; Miller, D. J.; Nordlund, D.; Ogasawara, H.; Nilsson, A. Degradation of Bimetallic Model Electrocatalysts: An In Situ X-Ray Absorption Spectroscopy Study. *Angew. Chem., Int. Ed.* **2011**, *50*, 10190–10192.

47 Peng, Z. M.; You, H. J.; Yang, H. An Electrochemical Approach to PtAg Alloy Nanostructures Rich in Pt at the Surface. *Adv. Funct. Mater.* **2010**, *20*, 3734–3741.

48 Srivastava, R.; Mani, P.; Hahn, N.; Strasser, P. Efficient Oxygen Reduction Fuel Cell Electrocatalysis on Voltammetrically Dealloyed Pt-Cu-Co Nanoparticles. *Angew. Chem., Int. Ed.* **2007**, *46*, 8988–8991.

49 Kijima, T. Inorganic and Metallic Nanotubular Materials: Recent Technologies and Applications. *Top. Appl. Phys.* **2010**, *117*, 215–234.

50 Chen, Z. W.; Waje, M.; Li, W. Z.; Yan, Y. S. Supportless Pt and PtPd Nanotubes as Electrocatalysts for Oxygen-Reduction Reactions. *Angew. Chem., Int. Ed.* **2007**, *46*, 4060–4063.

51 Liu, L. F.; Pippel, E. Low-Platinum-Content Quaternary PtCuCoNi Nanotubes with Markedly Enhanced Oxygen Reduction Activity. *Angew. Chem., Int. Ed.* **2011**, *50*, 2729–2733.

52 Tao, F.; Grass, M. E.; Zhang, Y. W.; Butcher, D. R.; Renzas, J. R.; Liu, Z.; Chung, J. Y.; Mun, B. S.; Salmeron, M.; Somorjai, G. A. Reaction-Driven Restructuring of Rh-Pd and Pt-Pd Core-Shell Nanoparticles. *Science* **2008**, *322*, 932–934.

53 Andersson, K. J.; Calle-Vallejo, F.; Rossmeisl, J.; Chorkendorff, L. Adsorption-Driven Surface Segregation of the Less Reactive Alloy Component. *J. Am. Chem. Soc.* **2009**, *131*, 2404–2407.

54 Wang, C.; Chi, M. F.; Li, D. G.; Strmcnik, D.; van der Vliett, D.; Wang, G. F.; Komanicky, V.; Chang, K. C.; Paulikas, A. P.; Tripkovic, D.; Pearson, J.; More, K. L.; Markovic, N. M.; Stamenkovic, V. R. Design and Synthesis of Bimetallic Electrocatalyst with Multilayered Pt-Skin Surfaces. *J. Am. Chem. Soc.* **2011**, *133*, 14396–14403.

55 Wang, D.; Xin, H. L.; Hovden, R.; Wang, H.; Yu, Y.; Muller, D. A.; DiSalvo, F. J.; Abruña, H. D. Structurally ordered intermetallic platinum−cobalt core−shell nanoparticles with enhanced activity and stability as oxygen reduction electrocatalysts. *Nat. Mater.* **2013**, *12*, 81–87.

56 Thorson, M. R.; Brushett, F. R.; Timberg, C. J.; Kenis, P. J. A. Design rules for electrode arrangement in an air-breathing alkaline direct methanol laminar flow fuel cell. *J. Power Sources* **2012**, *218*, 28–33.

57 Garsany, Y.; Baturina, O. A.; Swider-Lyons, K. E.; Kocha, S. S. Experimental Methods for Quantifying the Activity of Platinum Electrocatalysts for the Oxygen Reduction Reaction. *Anal. Chem.* **2010**, *82*, 6321–6328.